David Lynn[1], Ted Steinberg[2], Kyle Sparks[3] and Joel M. Stoltzfus[4]

Defining the Flammability of Cylindrical Metal Rods Through Characterisation of the Thermal Effects of the Ignition Promoter

---

ABSTRACT: All relevant international standards for determining if a metallic rod is flammable in oxygen utilise some form of “promoted ignition” test. In this test, for a given pressure, an overwhelming ignition source is coupled to the end of the test sample and the designation flammable or non-flammable is based upon the amount burned, that is, a burn criteria. It is documented that 1) the initial temperature of the test sample affects burning of the test sample both a) in regards to the pressure at which the sample will support burning (threshold pressure) and b) the rate at which the sample is melted (regression rate of the melting interface) and, 2) the igniter used affects the test sample by heating it adjacent to the igniter as ignition occurs. Together, these facts make it necessary to ensure, if a metallic material is to be considered flammable at the conditions tested, that the burn criteria exclude any region of the test sample that may have undergone preheating during the ignition process. A two-dimensional theoretical model was developed to describe the transient heat transfer occurring and resultant temperatures produced within this system. Several metals (copper, aluminum, iron and stainless steel) and ignition promoters (magnesium, aluminum and Pyrofuze ®) were evaluated for a range of oxygen pressures between 0.69 MPa (100 psia) and 34.5 MPa (5000 psia). A MATLAB ® program was utilised to solve the developed model that was validated against 1) a published solution for a similar system and 2) against experimental data obtained during actual tests at NASA WSTF. The validated model successfully predicts temperatures within the test samples with agreement between model and experiment increasing as test pressure increases and/or distance from the promoter increases. Oxygen pressure and test sample thermal diffusivity were shown to have the largest effect on the results. In all cases evaluated, there is no significant preheating (above about 38^{o}C/100^{o}F) occurring at distances greater than 30 mm (1.18 in.) during the time the ignition source is attached to the test sample. This validates a distance of 30 mm (1.18 in.) above the ignition promoter as a burn length upon which a definition of flammable can be based for inclusion

in relevant international standards (that is, burning past this length will always be independent of the ignition event for the ignition promoters considered here).

KEYWORDS: promoted ignition, metal combustion, heat conduction, thin fin, promoted combustion, burn length, burn criteria, flammability, igniter effects, heat affected zone

---

[1]PhD candidate, School of Engineering Systems, Queensland University of Technology, GPO Box 2434, Brisbane, 4001, Queensland, Australia

[2]Professor, School of Engineering Systems, Queensland University of Technology, GPO Box 2434, Brisbane, 4001, Queensland, Australia

[3]NASA Test and Evaluation Contract, NASA White Sands Test Facility, Las Cruces, New Mexico, USA

[4]Special Program Manager, NASA White Sands Test Facility, Las Cruces, New Mexico, USA

INTRODUCTION

A number of test methods are currently used to evaluate the flammability of metallic materials, including those developed by NASA [1], ASTM [2] and ISO [3]. In each of these tests, a cylindrical rod of length, *L,* and radius, *R*,* is vertically mounted in a test chamber and ignited at the bottom-end, typically through the use of an ignition promoter that is resistively heated to initiate burning. The promoter heats the end of the test sample to its melting point then detaches (melts off) from the sample. The material is considered flammable, under the specific environmental conditions being evaluated, if the burning continues after the effects of the igniter are dissipated. This burning independent of the igniter is historically indicated by the sample burning more than some predefined length (that is, burning continues along the test sample for more than some arbitrary length).

The particular method of ignition used, however, means that during the ignition process energy is transferred to the test material, resulting in some pre-heating of the sample. Past work [4, 5] has demonstrated that an increase in test sample temperature can potentially affect the flammability of a test sample and the rate at which the sample is consumed, that is, raising the initial temperature of the sample can lead to the sample burning at a lower test pressure and being consumed (burning) faster. Additionally, the material properties of the test sample being evaluated, as well as the different characteristics of the various promoter types typically used, will influence the results obtained (that is, the extent of the test sample that is preheated by the igniter). Since these standard tests are commonly used to relatively rank different metallic materials, dissimilar thermal diffusivities of the test material (for a similar igniter) will lead to differences in the extent of the preheated zone and could, therefore, potentially change the ranking of one metallic material relative to another. These reasons make it necessary to ensure that any definition of flammability that is used based upon a test sample's burn length preclude any region that is preheated by the promoter during the ignition process.

The work presented here outlines the development of a theoretical model and numerical simulation using MATLAB ® to predict the temperature distribution in a test sample as a result of pre-heating by the igniter. Based on this model, a prediction of the transient heat transfer that occurs during the ignition process is made. The objective of the current work is to validate the developed model and then characterise the resulting temperature distribution produced in the test sample from the ignition promoter. Characterisation of this resultant temperature distribution is then used to provide a definition of when a sample can be considered flammable (i.e. it is burning independent of the igniter used) for incorporation into relevant international standards.

BACKGROUND

According to all the relevant international standards in this area, for a test sample to be considered flammable, under the specific environmental conditions being evaluated, the burning must be “self-sustaining”. Currently, the NASA test specifies this is true if one (of 10) specimen burns more than 30 mm (1.18 in.) (for a sample that is at least 102mm (4 in.) pre-test length), the ISO test specifies this is true if one (of 10) specimen burns more than half way (150 mm for a sample that is 305 mm pre-test length) and the ASTM test specifies this is true if complete consumption of the sample (up to the sample holder) occurs in at least one (of 5) test (for samples that are ~150 mm pre-test length). These burn lengths were arbitrarily chosen and a goal of the current work is to better characterise the actual length a test sample needs to be consumed for the burning to be considered self-sustaining (and, therefore, the sample to be considered flammable by a standard test). The ASTM test standard is, as a matter of course, currently being reviewed and updated, with some focus on clarifying the true length a test sample must burn for it to be considered flammable; that is, burning independent of the ignition event.

The general burning characteristics of metals subjected to promoted ignition testing have been the focus of numerous studies. Past work has typically used two parameters, the Threshold Pressure (TP) and Regression Rate of the Melting Interface (RRMI) to characterise a metallic material’s propensity to support burning under a given set of experimental conditions. The TP is the lowest

pressure (of those tested) that will support burning of a sample and the RRMI is the rate at which the melting interface (surface between the liquid molten ball formed on the end of the rod during burning and the solid metal rod) moves along the rod while burning. These parameters provide an indication of a metallic material's absolute and relative flammability making comparisons between different metals possible.

In particular, the Heat Affected Zone (HAZ), and other thermal effects produced by the igniter have received some, albeit limited, attention. Figure 1 shows a typical test sample, post-test, and how conductive heating affects the sample internally. Previous work has shown that metallic material flammability is directly affected by the temperature of the sample being tested [6-13]. One limited study has suggested that no significant pre-heating effects are present further than ~ 20-30 mm from the base of the sample (see Figure 2b) [14]. There are, however, limited experimental or theoretical results available to indicate the exact effect of temperature on metallic material flammability [8-13]. The limited results available use TP and RRMI as indicators of the effects of temperature on burning. This past work shows that, in general, an increase in the temperature of the test sample results in an increase in the RRMI [8, 10-13] and a decrease in the TP [8, 9, 13]. Though these are the general trends reported on in these publications, it is very important to note that these changes in TP and RRMI were not (given the limited data presented) observed for relatively minor increases in sample temperature (e.g. 100 ^{o}C – 250 ^{o}C (210-480 ^{o}F)), rather they were observed for major increases in the test samples ambient temperature (often temperature values much greater than 250 ^{o}C – 300 ^{o}C (480-570 ^{o}F)).

THEORETICAL DESCRIPTION

The transient heat transfer occurring in a cylindrical-pin fin is of interest in a number of applications. Chapman, cited in [15], initially examined the transient heat transfer in annular fins. Yang [16] and Aziz [17] then examined the heat transfer occurring in straight and annular fins, respectively, with both fins exposed to a periodic variation in base temperature. Chu et al. [15] performed a two dimensional analysis of cylindrical-pin fins, and these studies enabled Su and Hwang [18, 19] to

extend the work to a two-dimensional model to account for convective effects from the pin sides and tip. Finally, Chang et al. [20] modified the model to allow for non-constant spatial and time boundary conditions occurring at the base of the pin fin.

The analytical solutions produced by Su and Hwang and Chang et al. respectively are slightly extended and used in the current work. The current work is solved by the combined method of separation of variables and principle of superposition. The resulting model produced describes the temperature distribution, as well as heat transfer along the test sample, as determined by a number of physically relevant boundary conditions and appropriate initial condition. These conditions and the final equations for this model are presented and discussed in more detail, along with the adaptation of the model to the system being studied in this work.

Figure 2 shows a schematic of the configuration of the cylindrical rod, as is typically used in the various standardised tests, and as is used in the theoretical model presented here.

Nomenclature

Bi_a	transversal Biot number $Bi_a = \frac{hR^*}{k}$
Bi_T	tip Biot number $Bi_T = \frac{h_T L}{k}$
L	cylindrical rod length
R^*	radius of cylindrical rod
R	dimensionless rod radius $(= R^* / L)$
G	geometry factor $(= L / R^*)$
h	convective heat transfer coefficient – lateral surface
h_T	convective heat transfer coefficient – tip
J_0	zero-order Bessel function
J_1	first-order Bessel function

k	thermal conductivity of test sample
$T^*(x^*, r^*, t^*)$	transient temperature
$T(x, r, t)$	dimensionless transient temperature $[= (T^*(x^*, r^*, t^*) - T_\infty^*)/(T_m^* - T_\infty^*)]$
T_∞^*	ambient chamber temperature
T_m^*	material melting temperature
t^*	time
t	dimensionless time $(= \alpha t^* / L^2)$
x^*, r^*	co-ordinate system (x is along rod and r is radial)
x, r	dimensionless co-ordinates $(x = x^* / L,\ r = r^* / L)$
α	thermal diffusivity of sample
η_n, β_m	n^{th} and m^{th} positive roots of transcendental equations, respectively

Assuming cylindrical symmetry, the equations describing the temperature distribution and heat transfer within the test system as well as the initial and boundary conditions for a constant base temperature are:

Two-dimensional heat transfer equation:

$$\frac{\partial T(t,x,r)}{\partial t} = \frac{\partial^2 T(t,x,r)}{\partial x^2} + \frac{\partial^2 T(t,x,r)}{\partial r^2} + \frac{1}{r}\frac{\partial T(t,x,r)}{\partial r} \tag{1}$$

Initial condition: $t = 0$

For all (x,r) $\quad T(0,x,r) = 0$ (2)

Boundary conditions: $t > 0$*;*

$x = 0$ $\qquad T(t,0,r) = 1$ (3a)

$x = 1$ $\qquad \frac{\partial T(t,1,r)}{\partial x} + Bi_T T(t,1,r) = 0$ (4)

$r = 0$ $\qquad \frac{\partial T(t,x,0)}{\partial r} = 0$ (5)

$$r = R \qquad \frac{\partial T(t,x,R)}{\partial r} + GBi_a T(t,x,R) = 0 \tag{6}$$

Equations 1-6 are solved by standard techniques to produce the solution for the time independent (base) boundary condition as shown in Equation 7. This is used to determine the temperature distribution found in the cylindrical test specimen at a specific time and location, (t, r and x) for specific material properties (α) and convective properties (h and h_T).

$$T(t,x,r) = \sum_{n=1}^{\infty} \frac{2Bi_a J_0(\eta_n Gr)}{(\eta_n^2 + Bi_a^2) J_0(\eta_n)} \times \left\{ \frac{\eta_n G \cosh[\eta_n G(1-x)] + Bi_T \sinh[\eta_n G(1-x)]}{\eta_n G \cosh(\eta_n G) + Bi_T \sinh(\eta_n G)} \right.$$

$$\left. - \sum_{m=1}^{\infty} \frac{2\beta_m^2 e^{-(\beta_m^2 + \eta_n^2 G^2)t} \sin(\beta_m x)}{(\beta_m^2 + \eta_n^2 G^2)[\beta_m - \cos(\beta_m)\sin(\beta_m)]} \right\} \tag{7}$$

The above solution is conditional on satisfying the following two transcendental functions:

$$\eta_n J_1(\eta_n) - Bi_a J_0(\eta_n) = 0 \tag{8}$$

$$\beta_m \cot(\beta_m) = -Bi_T \tag{9}$$

It is only the preheating of the sample rod during the ignition stages of a test that is of relevance in this work, thus making the time an ignition promoter is burning an important parameter in the model. It is during this critical “igniter burn time” (t_{crit}), that the bottom of the sample rod undergoes a rapid rise in temperature from ambient to melting temperature (corresponding to the specific test material being evaluated). Promoted ignition tests have demonstrated that, depending upon the promoter used (aluminum, magnesium or Pyrofuze ® igniter wire) and the gas pressure of the test environment, t_{crit} can vary from between approximately 0.1 s up to about 0.6 s [21]. During this initial t_{crit}, the base temperature of the test sample is modelled to vary exponentially with time between the ambient temperature and the material melting temperature, and is approximated by setting the dimensionless base temperature boundary condition (Equation 3) to be equal to:

$$x = 0 \qquad T(t,0,r) = 1 - e^{-bt} \tag{3b}$$

where, b is a suitable time constant such that the base reaches roughly the sample’s melting temperature over the time period, t_{crit}.

Using Duhamel's method (see [22]), the solution for a time dependent (base) boundary condition can be expressed as in Equation 10, in agreement with the work of Chang et al [20].

$$T(t,x,r) = T(0)\phi(t,x,r) + \int_{\tau=0}^{t} \frac{dT(\tau)}{d\tau}\phi(t-\tau,x,r)d\tau \tag{10}$$

where, $\phi(t,x,r)$ represents the *time independent* solution, as found in Equation 7, and the time dependent functions are evaluated at a fixed time $t = \tau$.

Applying the exponential boundary condition (Equation 3b) and substituting Equation 7 into Equation 10, yields:

$$T(t,x,r) = \sum_{n=1}^{\infty}\left[\frac{2Bi_a J_0(\eta_n G r)}{(\eta_n^2 + Bi_a^2)J_0(\eta_n)}\right]\left\{[1-e^{-bt}]\left[\frac{\eta_n G\cosh[\eta_n G(1-x)] + Bi_T \sinh[\eta_n G(1-x)]}{\eta_n G\cosh(\eta_n G) + Bi_T \sinh(\eta_n G)}\right]\right.$$

$$\left. -\sum_{m=1}^{\infty}\left[\frac{2\beta_m^2 e^{-(\beta_m^2+\eta_n^2 G^2)t}\sin(\beta_m x)}{(\beta_m^2+\eta_n^2 G^2)[\beta_m - \cos(\beta_m)\sin(\beta_m)]}\right]\left[\frac{b}{b-(\beta_m^2+\eta_n^2 G)}[e^{-(\beta_m^2+\eta_n^2 G^2)t} - e^{-bt}]\right]\right\} \tag{11}$$

Equation 11 specifies the temperature distribution in the cylindrical test specimen for a given location, at a given time for specific material properties (α) and convective properties (h and h_T). From this system of equations, appropriate boundary and initial conditions, the temperature at a given time and point within or on the cylindrical test-piece can be specified (and compared to experimental measurements).

MODEL SOLUTION

A model has been developed to describe the transient heat transfer along a cylindrical metallic "pin fin" caused by promoted ignition at the beginning of an experiment. This model is used to provide the temperature distribution along the rod during the ignition process prior to the test sample burning in an ongoing fashion.

From Equation 11, it can be seen that to solve for a given temperature, two infinite sums need to be determined. As a result, a convergence criteria needs to be specified. To replicate the process

used by Su and Hwang [18], the summing process was terminated when the absolute value of the last term in the series was less than $1x10^{-6}$.

The presence of the hyperbolic cosines in the equations produced exceptionally large numbers (>>$1.78x10^{308}$) which necessitated the use of the Symbolic Math Toolbox™, since normal MATLAB ® floating point precision can handle only numbers of absolute magnitude less than approximately $1.78x10^{308}$. This Symbolic Math Toolbox™ allows the use of variable precision accuracy, in turn allowing the developed set of equations to be readily solved.

Using the developed model, and the thermophysical parameters of a given test material and environmental conditions present, the system allows the prediction of the temperature distribution and transient heat transfer characteristics within the test sample. Figure 3 shows the MATLAB® solution of the developed equations, compared to the results of Su and Hwang [9, 10].

As Figure 3 shows, the surface temperature distribution produced by the MATLAB® model in the present work is in excellent agreement with the previously published work, confirming the validity of the program and solution approach allowing it to be applied to the rod ignition phenomena being studied here.

EXPERIMENTAL SYSTEM

To further validate the model, experimental work was conducted to allow comparison of model predictions to actual temperatures recorded along a sample rod while ignition occurs at the bottom of the sample. The experimental work was conducted at NASA White Sands Test Facility (WSTF) [14]. Temperature measurements were obtained from a number of thermocouples placed at varying intervals along the rod. Figure 2b shows a typical experimental thermocouple configuration utilised.

Two sets of experimental data are shown in Figure 4 describing the temperature at each of the thermocouples (shown in Figure 2b), for a copper rod with a magnesium and aluminum promoter in 34.5 MPa (5000 psia) oxygen and 3.45 MPa (500 psia), respectively. For the higher pressure case (34.5 MPa/5000 psia), there is little heating of the test sample evidenced above about 10 mm (0.4 in.) from the top of the promoter. However, for the lower pressure case (3.45 MPa or 500 psia) some preheating of the sample occurs, though significant preheating effects (heating to > 150^{o}C (~ 300^{o}F)) are only recorded in the 12-17 mm (0.6-0.8 in.) closest to the top of the promoter. Above this position (12-17 mm, 0.6-0.8 in.), there is negligible heating of the test sample from the ignition event.

RESULTS AND DISCUSSION

The experimental work included three metal test samples (copper, Monel 400 and 316 Stainless steel), three igniter materials (Pyrofuze ®, aluminum and magnesium though most testing was only performed with aluminum and magnesium promoters), and four test pressures (0.69 MPa/100 psia, 3.45 MPa/500 psia, 6.9 MPa/1000 psia, and 34.5 MPa/5000 psia). These test materials provide a good range of thermal diffusivities and the ignition promoters provide a good range of t_{crit}'s thus allowing a robust validation of the model's predictions. Table 1 provides the thermophysical parameters used for each material in the model to generate the theoretical results.

The ignition promoter used and the gas pressure of the test environment have been observed to effect the length of the ignition period, t_{crit} [4, 14]. A table of typical t_{crit} values as a function of these parameters, used in the solution of the theoretical model to compare to the experimental measurements, is provided in Table 2. These values are obtained through experimental observations. As expected, as the pressure increases, the t_{crit} value decreases. Also, due to its low mass, when using just the Pyrofuze ® igniter wire, a relatively faster burn time at a given pressure than either the aluminum or magnesium igniters is observed.

Figure 4 shows a comparison of model predictions to experimental results for a (3.2 mm (0.125 in.) diameter) copper test sample in a) 34.5 MPa/5000 psia oxygen with a magnesium promoter and b) 3.45 MPa/500 psia oxygen with an aluminum promoter, respectively. There is little radial variation in temperature within the rod and the figure shown is for the predicted surface temperature on the rod (at r=R). Also indicated on Figure 4 is the time the promoter burned, (for the pressure the test was conducted at) t_{crit}, as given in Table 2. As can be seen from these figures, except for the thermocouple immediately adjacent to the ignition promoter, there is good agreement between the experimental results and the model predictions. Additionally, agreement between the model and the experimental results clearly increases with distance from the promoter. In all cases evaluated here, excellent agreement is obtained between model and experiment for distances greater than approximately 14 mm (0.6 inches) from the top of the promoter.

The poor agreement between the model predictions and experimental measurements for the thermocouple closest to the promoter, and to a lesser extent the other thermocouples, is likely due to a number of real effects that are not incorporated in the theoretical model. These effects include (in perceived order of importance): 1) The use of constant convective heat transfer coefficients (h and h_T) along/on the end of the test sample. Clearly evidenced from the video recordings of the results is the fact that during the ignition of the promoter, large convective mixing is induced; it is not uniform over the length of the test sample, and this mixing is most pronounced near the bottom of the sample (where the promoter is located). 2) The use of constant thermophysical parameters in the model (that is, the use of average material properties not changing with temperature or pressure). This would include the conductivities, densities and specific heats (and hence, thermal diffusivities) for the metals. 3) Non-uniform burning of the promoters. When a promoter is ignited it is assumed it is burning uniformly. The model averages this effect out by considering the heating of the promoter region from ambient to the rod's melting point to occur over the time, t_{crit}. 4) Not accounting for the physical interaction of the burning promoter and end of test sample that is being melted. 5) Noting that the thermocouples are actually just below the surface of the test sample at different depths (but are compared to model predictions for the surface). Because of these effects, agreement between the model and the experimental measurements in the region immediately

adjacent (above) the promoter would be expected to be (and is) limited. However, model predictions and experimental measurements are in good agreement and consistent above a small region (~14 mm) just adjacent to the promoter and it here that the model can be applied and is useful in determining what region of the test sample is within the HAZ while the promoter is still attached. Clarification of the extent of this HAZ will assist in defining when a sample is flammable (that is, ongoing burning independent of the ignition event).

These results validate the predictions of the thermal model developed, especially at distances greater than 14 mm (0.6 inches) above the promoter. Further presentation and discussion of the experimental results obtained during this program and their meaning is provided in the publication by Sparks et al. [14]. The model can be used to predict (for many different sample materials, test pressures and igniter types examined here) the approximate extent of the HAZ produced while the promoter is melting the end of the test sample. The extent of this HAZ can then be used (coupled with a factor-of-safety if required) to develop a definition of flammability that is independent of the ignition event and any associated heating of the test sample. That is, if a test sample burns a distance greater than the extent of the HAZ produced by the promoter, it can be considered to be burning independent of the ignition event and, conversely, a test sample that burns a distance less than this value cannot be considered to be flammable.

As stated, the model can be used to study the effects of various sample and environmental properties on the extent of the HAZ produced during ignition of the test samples. Of particular interest here is how far up the rod the preheating occurs and how the extent of the HAZ changes with the material thermal diffusivity. Figures 5-7 show, for a test sample in oxygen at 0.69 MPa (100 psia), 3.45 MPa (500 psia) and 34.5 MPa (5000 psia), a comparison of the temperature within the test sample at 15 mm (0.59 in.) and 30 mm (1.18 in.) above the promoter, respectively, for the metallic materials given in Table 1. These figures provide a good range of thermal diffusivities typically encountered and confirm that, since few metallic materials have a higher thermal diffusivity than copper (and none significantly so), estimates for the extent of the HAZ will be largest when they are based on a copper test sample.

As expected, and clearly illustrated in Figures 5-7 above: 1) As test pressure increases, (the burning time of the promoter is shorter (t_{crit}) and, the preheating effects within the test sample decrease, that is, there is a smaller HAZ created within a test sample at higher pressures, 2) as the thermal diffusivity of the metal sample increases, the extent of the HAZ increases, and 3) if general estimates are to be made regarding the extent and magnitude of the HAZ, a low oxygen test pressure combined with a test material with a high thermal diffusivity should be used.

Figure 7 shows that at 34.5 MPa (5000 psia), for all of the materials considered here, there are no heating effects within the test sample from the ignition above about 15 (~0.59 in.) mm from the top of the promoter. Figure 6 shows that at 3.45 MPa (500 psia), for all of the materials considered here, there are no heating effects within the test sample from the ignition above about 30 mm (1.18 in.) from the top of the promoter. However, for tests at 3.45 MPa (500 psia) the sample rod was found to reach between 90-150^{o}C (~200-300^{o}F) at a distance of 15mm (0.59 in.) from the top of the promoter (during the ignition period), depending upon the thermal diffusivity of the sample rod. Figure 5a shows that at low pressures (0.69 MPa/100 psia) at 15 mm (0.59 in.) above the top of the promoter, there is significant heating of the test sample occurring for both the copper (up to ~232^{o}C/450^{o}F) and aluminum (up to ~121^{o}C/250^{o}F) samples while the promoter is burning (up to t_{crit}=0.75 s). However, Figure 5b shows that at 30 mm (1.18in) above the top of the promoter, there is no significant heating (<38^{o}C/100^{o}F) of the test sample (at those same low pressures (0.69 MPa/100 psia)) occurring for any of the metals considered.

Using the results for copper (high thermal diffusivity) at low pressure (0.69 MPa/100 psia) provides the “worst-case” estimates for the extent of the HAZ produced by an ignition promoter while attached to the end of the test sample. These results clearly indicate that for all metal test samples considered (copper, aluminum, iron, stainless steel), for all promoters evaluated (Pyrofuze ®, magnesium, aluminum), and for test pressures over 0.69 MPa (100 psia) the HAZ produced is restricted to a region within about 30 mm (1.18in.) from the top of the promoter. That is, no heating above about 38 ^{o}C (100 ^{o}F) will occur within a test sample for any combination of these parameters

while the promoter is attached. As stated earlier, for the limited experimental data available, no changes in either TP or RRMI are expected for a material preheated to this level (or even twice this temperature). This implies any burning of a standard test sample for more than 30 mm (1.18 in) is the result of self-sustained burning independent of the ignition event for the promoter types investigated.

CONCLUSIONS

A two-dimensional theoretical model was developed to describe the transient heat transfer occurring and resultant temperatures produced within a cylindrical metal rod when an ignition promoter is ignited on the bottom of the rod in gaseous oxygen. Several metals (copper, aluminum, iron and stainless steel) and promoters (magnesium, aluminum and Pyrofuze ®) were evaluated for a range of oxygen pressures between 0.69 MPa (100 psia) and 34.5 MPa (5000 psia). A MATLAB ® program was utilised to solve the developed model that was validated against 1) a published solution for a similar system and 2) against experimental data obtained during actual tests at NASA WSTF. The validated model successfully predicts temperatures within the test samples with agreement between model and experiment increasing as test pressure increases and/or distance from the promoter increases. Oxygen pressure and test sample thermal diffusivity were shown to have the largest effect on the results with increases in sample thermal diffusivity or decreases in oxygen pressure producing a larger HAZ within the test sample. In all cases evaluated, there is no significant preheating (above about $38^{o}C/100^{o}F$) occurring at distances greater than 30 mm (1.18 in.). This validates a distance of 30 mm (1.18 in.) above the ignition promoter as a burn length upon which a definition of flammable can be based for inclusion in relevant international standards (that is, burning past this length will always be independent of the ignition event for the ignition promoters considered here).

REFERENCES

[1] *Flammability, Offgassing, and Compatibility Requirements and Test Procedures for Materials in Environments that Support Combustion*, Interim NASA Technical Standard NASA-STD-(I)-6001A (Previously NHB 8060.1C), National Aeronautics and Space Administration, 2008.

[2] "G124: Standard Test Method for Determining the Combustion Behaviour of Metallic Materials in Oxygen-Enriched Atmospheres," *ASTM Standards Related to Flammability and Sensitivity of Materials in Oxygen-Enriched Atmospheres,* American Society of Testing and Materials, Philadelphia, 1995.

[3] *Space Systems - Safety and Compatibility of Materials - Part 4: Determination of upward flammability of materials in pressurized gaseous oxygen or oxygen-enriched environments*, ISO 14624-4, International Organization for Standardization (ISO), 2003.

[4] Steinberg, T. A., "Metals Combustion at High-Pressure Oxygen in Normal and Reduced Gravity: Model and Experiment", PhD Thesis, New Mexico State University, Las Cruces, NM, 1990.

[5] De Wit, J. R., Steinberg, T. A., and Stoltzfus, J. M., "Igniter Effects on Metals Combustion Testing," *Flammability and Sensitivity of Materials in Oxygen-Enriched Atmospheres: Ninth Volume, ASTM STP 1395*, T. A. Steinberg, B. E. Newton, and H. D. Beeson Eds., American Society for Testing and Materials, West Conshohocken, PA, 2000, pp 190-203.

[6] Zaweirucha, R. and Million, J. F., "Promoted Ignition-Combustion Behaviour of Engineering Alloys at Elevated Temperatures an Pressures in Oxygen Gas Mixtures " *Flammability and Sensitivity of Materials in Oxygen-Enriched Atmospheres: Ninth Volume, ASTM STP 1395*, T. A. Steinberg, B. E. Newton, and H. D. Beeson Eds., American Society for Testing and Materials, West Conshohocken, PA, 2000, 119-133.

[7] Sato, J. and Hirano, T., "Fire Spread Limits along metal pieces in oxygen," *Flammability and Sensitivity of Materials in Oxygen-Enriched Atmospheres: Third Volume, ASTM STP 986*, D. W. Schroll Ed., American Society for Testing and Materials, Philadelphia, 1988, 158-173.

[8] Engel, C. D., Herald, S., and Davis, E., "Promoted Metals Combustion at Ambient and Elevated Temperatures," *Flammability and Sensitivity of Materials in Oxygen-Enriched Atmospheres: Eleventh Volume, ASTM STP 1479*, D. B. Hirsch, R. Zawierucha, T. A. Steinberg, and H. M. Barthelemy Eds., ASTM International, West Conshohocken, PA, 2006, pp. 51-61.

[9] Slockers, M. J. and Robles-Culbreth, R., "Ignition of Metals at High Temperatures in Oxygen," *Flammability and Sensitivity of Materials in Oxygen-Enriched Atmospheres: Eleventh Volume, STP 1479*, D. B. Hirsch, R. Zaweirucha, T. A. Steinberg, and H. M. Barthelemy Eds., ASTM International, Weston Conshohocken, PA, 2006, pp. 62-79.

[10] Sato, J., "Fire Spread Rates along Cylindrical Metal Rods in High Pressure Oxygen," *Flammability and Sensitivity of Materials in Oxygen-Enriched Atmospheres: Fourth Volume, ASTM STP 1040*, J. M. Stoltzfus, F. Benz, and J. S. Stradling Eds., American Society of Testing and Materials, West Conshohocken, PA, 1989, pp. 162-177.

[11] Sato, J. and Hirano, T., "Behaviour of Fires Spreading Along High-Temperature Mild Steel and Aluminum Cylinders in Oxygen," *Flammability and Sensitivity of Materials in Oxygen-Enriched Atmospheres: Second Volume, ASTM STP 910*, M. A. Benning Ed., American Society of Testing and Materials, Philadelphia, 1986, pp. 118-134.

[12] Benz, F. J., Shaw, R. C., and Homa, J. M., "Burn Propagation Rates of Metals and Alloys in Gaseous Oxygen," *Flammability and Sensitivity of Materials in Oxygen-Enriched Atmospheres: Second Volume, ASTM STP 910*, M. A. Benning Ed., American Society for Testing and Materials, Philadelphia, 1986, pp. 135-152.

[13] ASTM Committee G4 High Temperature Metals Combustion Test Program, *Personal Communication*, 2008.

[14] Sparks, K., Stoltzfus, J. M., Lynn, D. B., and Steinberg, T. A., "Determination of Pass/Fail Criteria for Promoted Combustion Testing," *Flammability and Sensitivity of Materials in Oxygen-Enriched Atmospheres: Twelfth Volume, ASTM STP xxxx*, Editors Ed., ASTM International, Location, 2009, pp. xx-xx.

[15] Chu, H. S., Chen, C. K., and Weng, C. I., "Transient Response of Circular Pins," *Journal of Heat Transfer,* vol. 105, 1983, pp. 205-208.
[16] Yang, J. W., "Periodic Heat Transfer in Straight Fins," *ASME Journal of Heat Transfer,* vol. 94, 1972, pp. 310-314.
[17] Aziz, A., "Periodic Heat Transfer in Annular Fins," *ASME Journal of Heat Transfer,* vol. 97, 1975, pp. 302-303.
[18] Su, R. J. and Hwang, J. J., "Transient Analysis of Two-Dimensional Cylindrical Pin Fin with Tip Convective Effects," *Heat Transfer Engineering,* vol. 20, 1999, pp. 57-63.
[19] Su, R. J. and Hwang, J. J., "Analysis of Transient Heat Transfer in a Cylindrical Pin Fin," *Journal of Thermophysics,* vol. 12, 1997, pp. 281-283.
[20] Chang, W., Chen, U., and Chou, H., "Transient Analysis of Two-Dimensional Pin Fins with Non-Constant Temperature," *JSME International Journal,* vol. 45, 2002, pp. 331-337.
[21] Steinberg, T. A., Wilson, D. B., and Benz, F. J., "Modeling of Al and Mg Igniters Used in the Promoted Combustion of Metals and Alloys in High Pressure Oxygen," *Flammability and Sensitivity of Materials in Oxygen-Enriched Atmospheres: Sixth Volume, ASTM STP 1197*, D. D. Janoff and J. M. Stoltzfus Eds., American Society of Testing Materials, Philadelphia, 1993, pp. 183-195.
[22] Carslaw, H. S. and Jaeger, J. C., *Conduction of Heat in Solids*, 2nd ed. London: Oxford University Press, 1959.
[23] NASA, "Evaluation of the zone that is heat-affected by standard promoters in metals testing," 2006, (Unpublished work).
[24] Davis, J. R., "Metals Handbook," 2nd ed., Materials Park, Ohio: ASM International, 1998.
[25] Peckner, D. and Bernstein, I. M., 2nd ed., "Handbook of Stainless Steels," New York: McGraw-Hill, 1977.

FIGURES

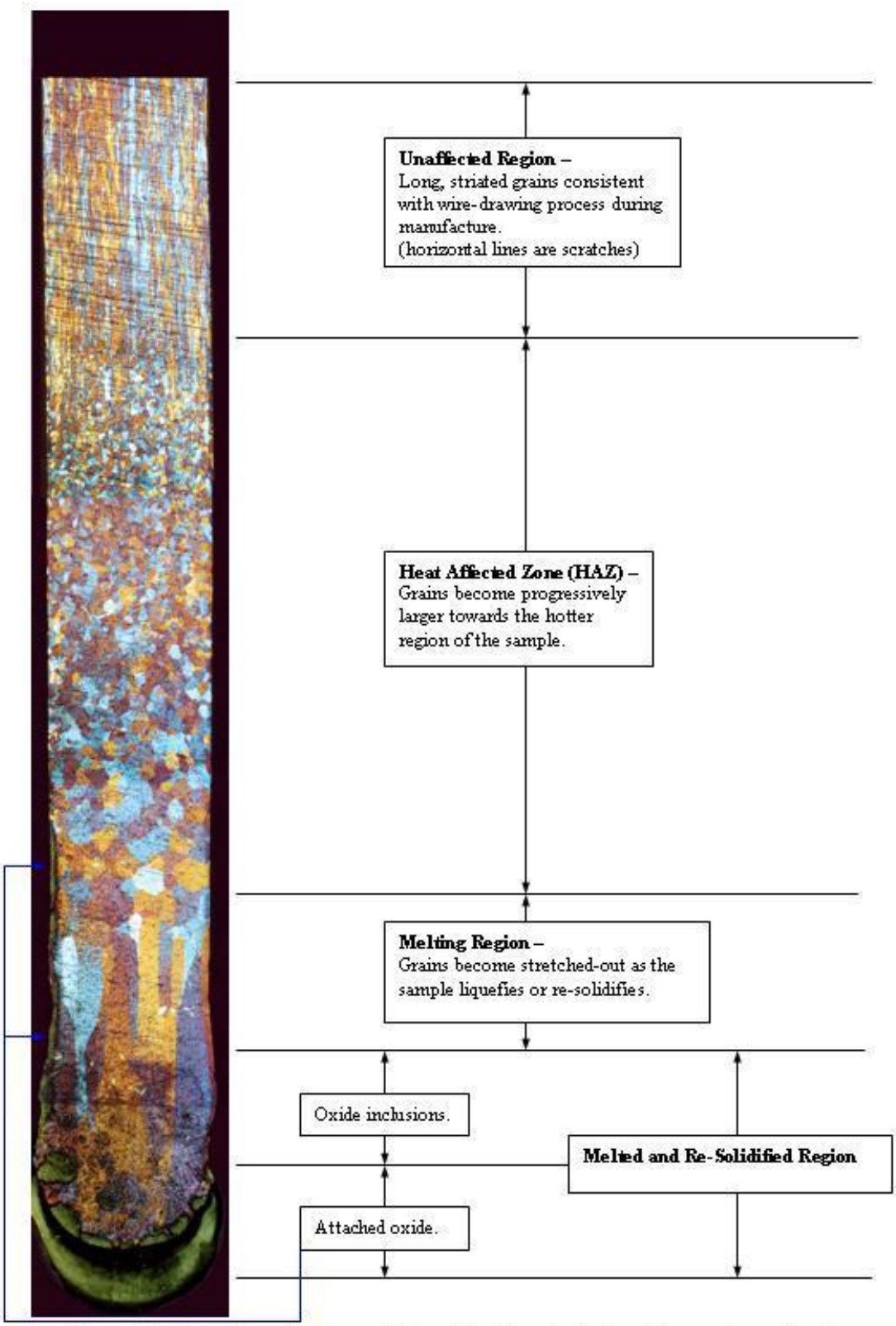

Figure 1. Cross-section of a typical 3.2mm (0.125 in.) diameter sample, post test [23].

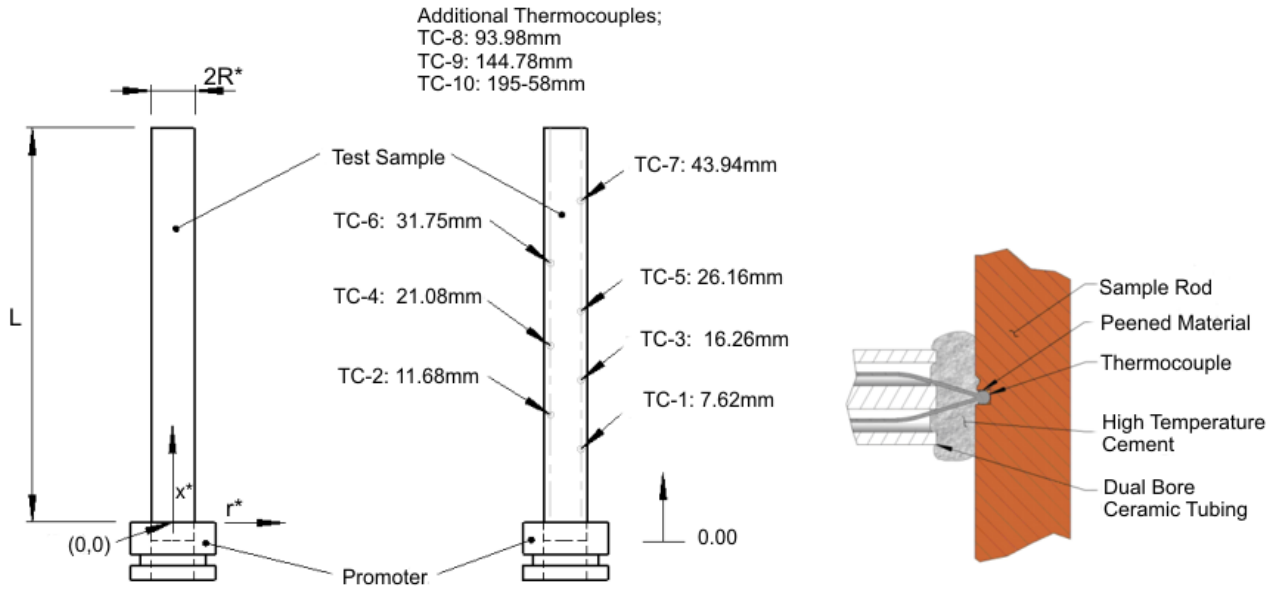

(a) (b) (c)

Figure 2. Schematic of sample configuration used in, a) model co-ordinate system, b) experimental configuration, c) thermocouple attachment.

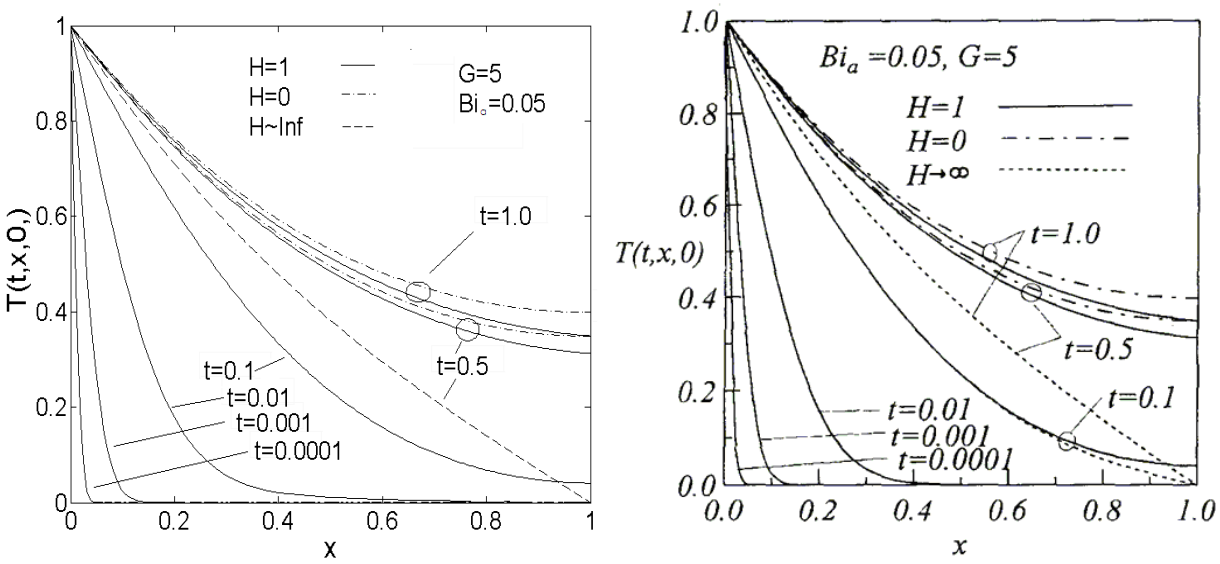

(a) (b)

Figure 3. Solution of developed model by (a) this work – MATLAB ® , and (b) Su and Hwang [18].

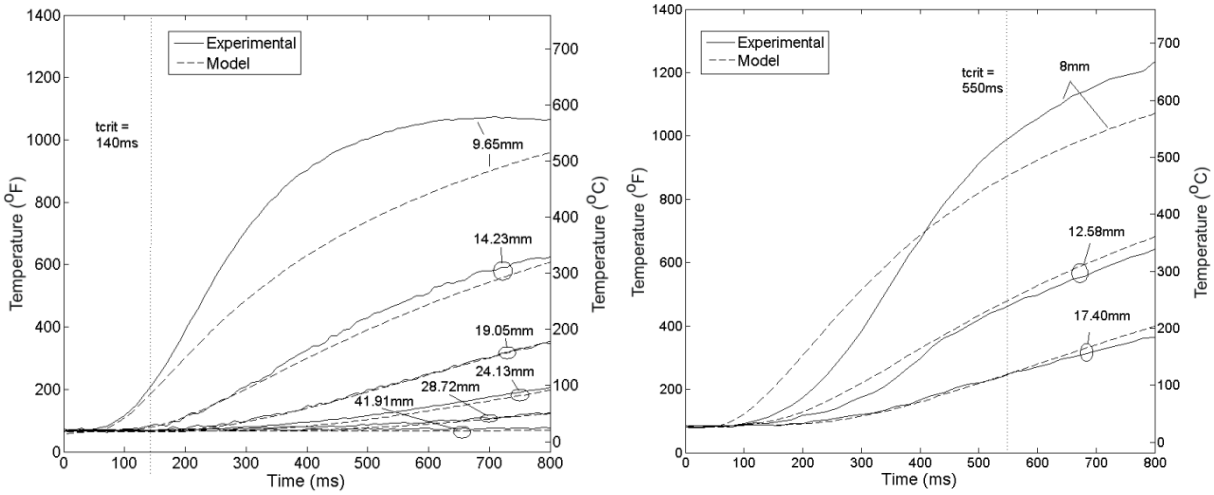

(a) (b)

Figure 4. Experimental versus model temperatures for a copper sample at (a) 34.5 MPa (5000 psia) with magnesium promoter and (b) 3.45MPa (500 psia) with aluminum promoter.

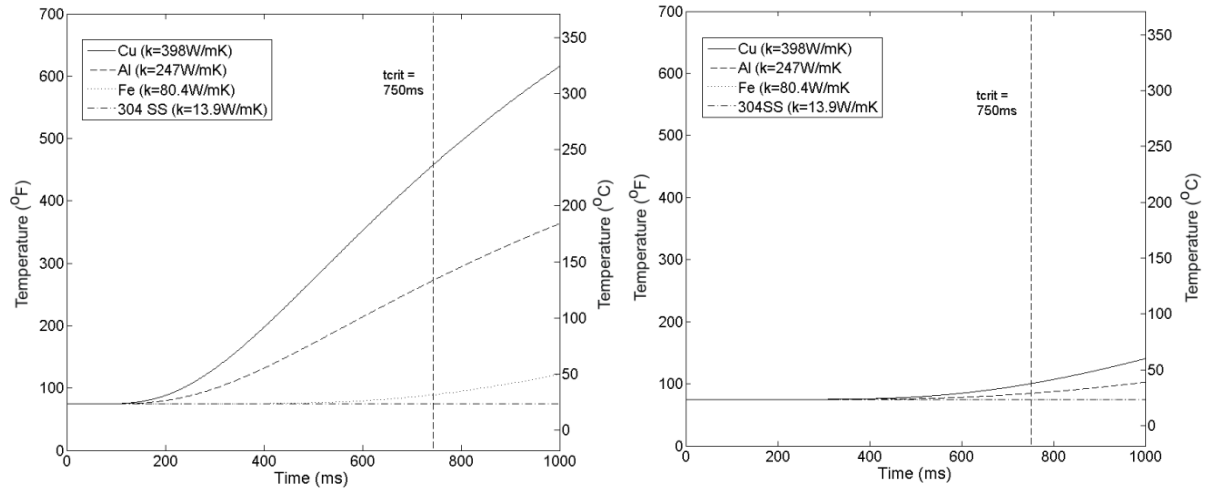

(a) (b)

Figure 5. Model temperatures predicted at (a) 15 mm (0.59 in.) and (b) 30 mm (1.18 in.) above promoter for 3.2 mm (0.125 in.) diameter copper, stainless steel, iron and aluminum test samples in 0.69 MPa (100 psia) oxygen (t_{crit} = 0.75 s).

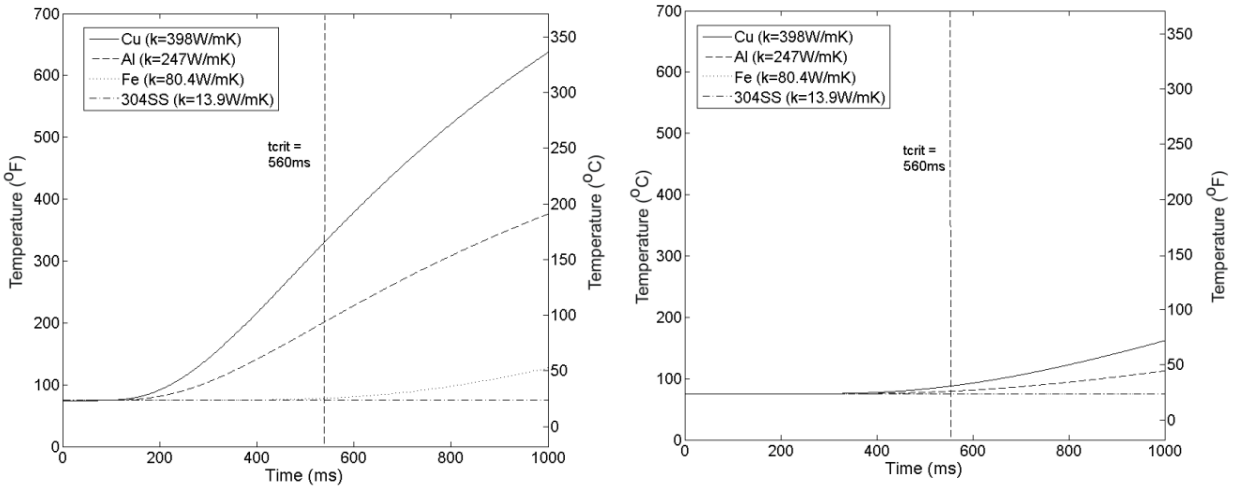

(a) (b)

Figure 6. Model temperatures predicted at (a) 15 mm (0.59 in.) and (b) 30 mm (1.18 in.) above promoter for 3.2 mm (0.125 in.) diameter copper, stainless steel, iron and aluminum test samples in 3.45 MPa (500 psia) oxygen (t_{crit} = 0.56 s).

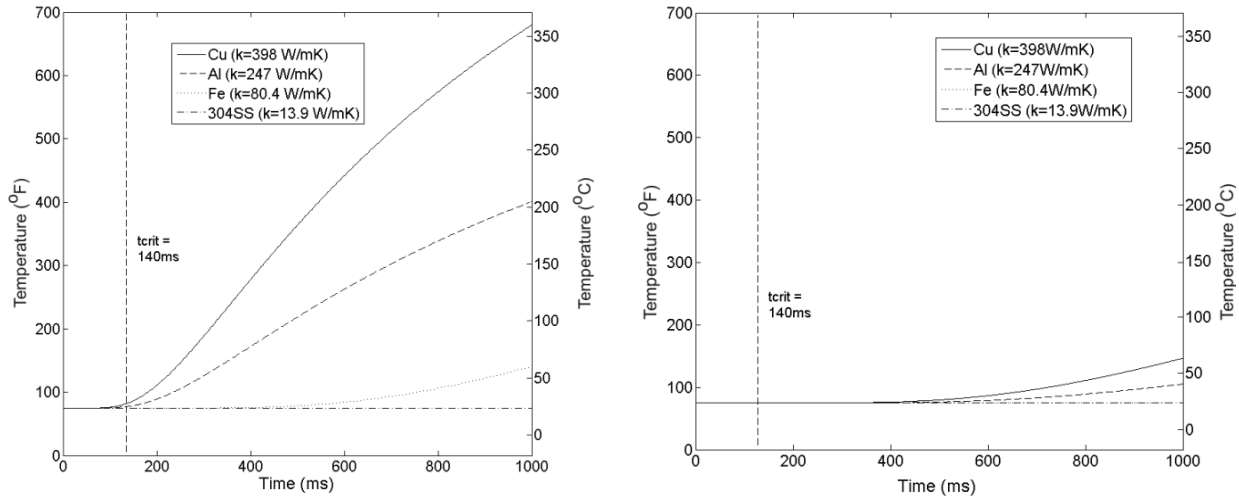

(a) (b)

Figure 7. Model temperatures predicted at (a) 15 mm (~0.59 in.) and (b) 30 mm (1.18 in.) above promoter for 3.2 mm (0.125 in.) diameter copper, stainless steel, iron and aluminum test samples in 34.5 MPa (5000 psia) oxygen (t_{crit} = 0.14 s).

Table 1. Summary of thermophysical properties used[1][24, 25].

Material/Chamber Property	**Cu**	**Al**	**Fe**	**304 SS**
Thermal Conductivity (k), W/mK, (BTUft/hrft^{2o}F)	398 (228)	247 (143)	80.4 (46.2)	13.9 (8.0)
Melting Point/Base Temperature ($T_0^* \approx T_m$), ^{o}C, (^{o}F)	1083 (1981)	657 (1215)	1538 (2800)	1398 (2550)
Density (ρ), kg/m^3, (lb/in^3)	8930 (0.323)	2699 (0.098)	7870 (0.284)	7700 (0.278)
Specific Heat (C_p) J/kgK, (BTU/lb^{o}F)	385 (0.092)	900 (0.215)	447 (0.107)	377 (0.09)
Thermal Diffusivity ($\alpha=k/C_p\rho$), m^2/s, (ft^2/s)	1.16×10^{-4} (1.23×10^{-3})	1.02×10^{-4} (1.09×10^{-3})	2.29×10^{-5} (2.44×10^{-4})	4.79×10^{-6} (5.14×10^{-5})
Convective Co-efficient – Lateral (h), W/m^{2}K, (BTU/hrft^{2o}F)	3.5 (0.616)			
Convective Co-efficient – Tip (h_T), W/m^{2}K, (BTU/hrft^{2o}F)	3.5 (0.616)			
Sample Length (L), m, (in)	0.3175 (12.5”)			
Sample Radius (s), m,(in)	0.0016 (0.063”)			

[1]The values used in Table 1 are approximated averages only; though they will vary with the changing temperature and pressure experienced by the sample, this variation is small and the average value shown in this table is the value used.

Table 2. Summary of t_{crit} values used in model as a function of promoter material and oxygen pressure.

PROMOTER MATERIAL	**t_{crit} (s) for igniter for different oxygen pressures - MPa (psia)**			
	0.69 (100)	**3.5 (500)**	**6.9 (1000)**	**35.0 (5000)**
magnesium	0.7	0.55	0.37	0.14
aluminum	0.8	0.57	0.37	0.14
Pyrofuze ®	--	0.20	--	--